Near Dry Powder Mixed Electric Discharge Machining of AA7050 Hybrid Composites Utilizing Composite Tool Materials

Poniface JOSE ALOYSIUS, Jacob Thambi Evans JEBEEN MOSES *, Varghese Thaya VIJUMON, Muthu Nadar FELIX XAVIER MUTHU

Department of Mechanical engineering, *St. Xavier's Catholic College of Engineering, Nagercoil -629003, Tamil Nadu, India*

http://doi.org/10.5755/j02.ms.34795

Received 5 August 2023; accepted 18 December 2023

Electric Discharge Machining (EDM) is a prominent technique for producing components with complex geometry and intricate shapes. However, productivity depends on the selection of optimal input variables. This research investigates EDM and Near-Dry EDM (NDEDM) on AA7050 hybrid composites, exploring the impact of tool materials, Al_2O_3 powder concentration, and dielectric fluids on Material Removal Rate (MRR) and Surface Roughness (R_a). NDEDM offers a higher MRR due to localized heating and energy concentration, while hydrocarbon oil EDM provides lower R_a due to cooling and lubrication. Tool material properties, thermal conductivity and bonding strength, affect MRR and TWR. Aluminum composite tools via stir casting display a strong bonding interface, leading to efficient energy transfer and higher MRR, while copper composite tools via friction stir processing exhibit weaker bonding, potentially reducing MRR. Hydrocarbon oil significantly lowers TWR due to effective lubrication and cooling, while near dry EDM results in slightly higher TWR. Al_2O_3 powder enhances MRR, with an optimal concentration of 1 g/l, while higher concentrations hinder MRR. The presence of Al_2O_3 powder enhanced the surface quality by reducing the size of the recast layers and producing a smoother surface. Globules, craters, microcracks, pock marks and re-casted layers are the noticeable features spotted on the surface. The results were optimized using the TOPSIS optimization technique and process parameters 32 A current, 30 µs Ton, 3 mm gap distance machined under 3 g/l Al_2O_3 incorporated hydrocarbon oil dielectric medium using copper composites tool proffers optimal machining performance.

Keywords: composite tools, near-dry electric discharge machining, electric discharge machining, stir casting, friction stir processing, TOPSIS.

1. INTRODUCTION

Conductive materials can be processed with electrical discharge machining regardless of their stiffness and mechanical attributes [1]. The method is based on striking the workpiece with countless minute electrical discharges from an electrode. Because each micro-electrical discharge melts a very small quantity of the metallic substance till the finished shape, complex structures may be made with dimensional tolerances of less than 50 µm [2]. Due to the requirement for great surface quality in intricately formed components in high-end applications like modern communications satellites, electro discharge machining becomes quite alluring [3]. Ten distinct die sink EDM input variables including current, voltage, Pulse on time, Pulse off time, flushing pressure were varied and machining efficiency was assessed in lexes of MRR, TWR and R_a. The results indicated that current was the most influential of all the selected input factors [4]. With the applied current, a plasma channel is generated in the spark gap, producing heat of extreme intensity that removes material through melting and evaporation [5]. Impacts of electrical input parameters on the effectiveness of the die-sinking electrical discharge machining process revealed that the discharge current and pulse length had a significant impact on MRR [6, 7].

The performance of the EDM machining is enhanced by adding foreign particles to the dielectric medium, graphite, aluminium oxide, boron carbide and silicon carbide are some of the predominantly used particles. Incorporating aluminium powder increases the MRR whereas blending graphite powder enhances surface quality [8]. The bridging effect is triggered by particle suspension, resulting in the development of intense heat, which enhances the MRR [9]. Powder mixed EDM reduces the recast layer of the machined surface. When tungsten particles are suspended in kerosene, discharges become steady and homogeneous, improving the surface finish [10]. Balbir Singh et al. blended tungsten powder of various particle sizes in dielectric fluid; the study revealed that the eradication of the recast layer improved surface quality. Also, the transfer of powder to the surface increased surface property [11]. Ramesh et al. EDMed Nimonic75 alloy by mixing Si, Mg and Gr powder in the dielectric medium. High MRR is provided by powder with high thermal conductivity, and it decreases as the weight % of particles increases [12].

Hydrocarbon oil, kerosine, oxygen, and paraffin are the distinct fluid used as the dielectric medium. The machining properties depend on the characteristics of the dielectric fluid. Biodegradable vegetable oils, such as jatropha, canola, and sunflower, exhibit similar dielectric characteristics to HCO and create an environmentally favourable condition [13]. Dielectric fluid with a high viscosity result in inadequate flushing of machined debris, which leads to the creation of a recast layer, which worsens

* Corresponding author. Tel.: +91-98436 25292.
E-mail: *jebeen@sxcce.edu.in* (J. Moses)

the surface quality [14]. Machined in the kerosene dielectric medium leads to the creation of titanium carbide and titanium oxide on the plane, requiring a high discharge energy and lowering machining performance [15]. Tap water has a higher MRR than distilled water, and surface cracks were caused by the rapid cooling rate when distilled water was employed as the dielectric fluid [16]. P. S. Ng et al. machined Bulk metal glass and titanium alloy using sunflower and canola biodiesel dielectric fluids. The findings showed that sunflower BD had a higher MRR and a lower TWR than conventional EDM oil [17]. Gases with low ionization energy and high electronegativity proffer the best machining performance owing to stabilized discharge [18]. Dry EDM gives a substantially lower TWR, but its low MRR prevents it from using non-oxygen gas in large quantities. To increase the MRR of dry EDM, the operating system uses piezoelectric gap control mechanisms, ultrasonic frequency actuators, and fluid dispersion phase in addition to the gas continuous phase [19]. The flow rate of powder-liquid mixtures, pulse on time, and peak current significantly affect the machining performance in near dry EDM [20]. The discharge is initiated by a solid liquid mixture, which dissipates heat by extending the plasma channel and flushes the machining debris due to the high explosive force [21].

Copper, brass, graphite, and aluminium are some of the EDM tool materials and machining characteristics depend on the electrical properties of the Tool [22]. Brass electrodes alloyed with zinc can reduce TWR and increase MRR, Copper tungsten composites have great tenacity when confronted with difficult workpiece materials, a characteristic widely coveted in the industrial industry [23, 24]. The effect of graphite's electrical conductivity emerges as a crucial component influencing both R_a and MRR [25]. A tool with a high melting temperature offers a lower TWR. Compared to other electrodes, the copper electrode has generated a smaller recast layer and reduced fracture width. [26]. The tool's resistance to electrical erosion is a function of both its mechanical and thermophysical characteristics. It was found that the composite electrodes with greater reinforcing percentages responded to pulse currents more favourably and generated more intense heat [27]. In the case of electrodes created by powder metallurgy, weekly bonded reinforced particles are deposited throughout the workpiece surface [28] and in the case of electrodes made by stir casting trigger a bridging effect [29]. Obtaining superlative from the available alternative is a perplexing task, TOPSIS, GRA, VIKOR and ELECTREE are some of the multi criteria decision making optimization techniques utilized for this purpose. R. Manivannan et al. utilize TOPSIS for optimizing the micro EDM of AISI 304 steel [30]. Using TOPSIS, Shailendra et al. computed the ideal turning parameters and found that the depth of cut, followed by feed rate and cutting speed, was the most crucial factor. Comparisons between the TOPSIS and GRA were performed, validation tests were steered to choose the best optimization approach [31, 32]. From the above survey it was clear that a lot of works were performed on EDM by altering parameters, tools, powder particles and dielectric fluid but no works were reported on composite tool as EDM that produced using the friction stir processing technique. In this work, an effort attempted to machine AA7050 hybrid composites by varying tool material viz Aluminium Composites (AC), Copper Composites (CC), Aluminium (A), Copper (C), electrical process parameters viz (current, gap distance and pulse on), Al_2O_3 powder concentration under HCO and near dry dielectric medium. The parameters were optimized using the TOPSIS technique and surface topography were machined using a Scanning Electron Microscope (SEM). The research objective is to evaluate the influence of various tool materials, including copper, aluminium, and composites fabricated through friction stir processing and stir casting, on the performance of EDM. The paper also intends to compare the efficacy of near-dry and hydrocarbon-based dielectric fluids in the EDM process.

2. MATERIALS AND METHODS

In this research, EDM and NDEDM were performed on AA7050 hybrid composites using an Elektra M2A Electric discharge machine by varying tool materials, Al_2O_3 powder concentration, gap distance, current and pulse on time and runs of experiments were planned utilizing L32 Taguchi mixed orthogonal as shown in Table 1. An attachment was designed and produced in-house to combine liquid and air, used as a dielectric in NDEDM. By combining liquid and air, this dielectric mixing device generates mist and is delivered through tubular electrodes between inter-electrode gaps, whereas EDM submerges the workpiece in HCO. The experiments were conducted for 10 mins, positive polarity was maintained and repeated three times. The MRR and TWR were determined according to Eq. 1 and Table 2 and R_a was measured using the SJ210 surface roughness tester. The surface topography was studied using the SEM and the parameter was optimized using TOPSIS. The tool material utilized for studies were copper composite reinforced with WC particles manufactured through Friction Stir Processing (FSP), aluminium composites processed through Stir Casting (SC), copper and aluminium tool of dimension 10 mm (ϕ) × 25 mm (L). The dimension of the EDM tool is depicted in Fig. 1.

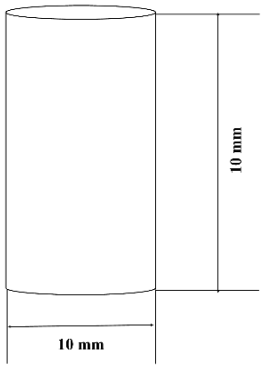

Fig. 1. Dimension of the EDM tool utilized for the study

WC particles of average particle size 5 μm as depicted in the Fig. 2 were selected as reinforcement owing to its high thermal conductivity (110 W/m-K) and high melting temperature (2780 °C), these properties facilitate dissipating heat generated during machining processes at lower TWR, which can be an advantageous factor for EDM. The FSP and SC process parameters was depicted in Table 2.

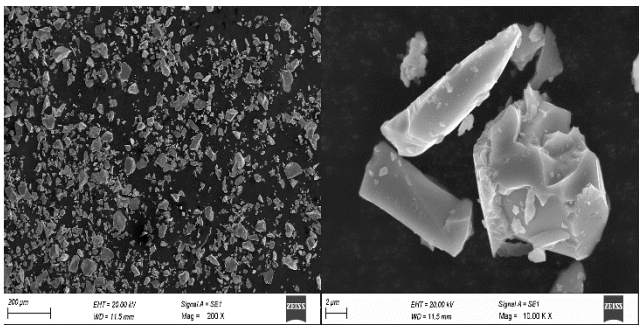

Fig. 2. SEM image showing the size of the WC particles

In the stir casting process, the alloy was melted in the graphite crucible to a temperature of 850 °C and stirred at the speed of 1000 rpm for 600 s utilizing a 3-arm mechanical stirrer. The WC of 5 wt.% was added to the melt and K_2TiF_6 flux was incorporated to improve the wettability and the mixture was down poured in a permanent die made of die steel. The FSP tool of 25 mm diameter shoulder, 10 mm diameter pin and a height of 10 mm rotated with a speed of 2000 rpm and a feed rate of 16 mm/min, at a 2° tilt angle. As the FSP tool traversed the workpiece, the heat generated due to the tool's high-speed rotation softened the copper matrix, allowing for the seamless mixing and dispersion of WC particles throughout the material. The schematic representation of SC and FSP setup is portrayed in Fig. 3.

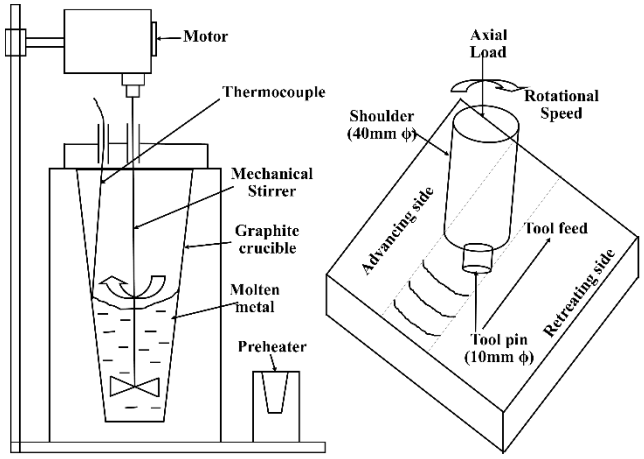

Fig. 3. Schematic representation of SC and FSP setup

$$MRR = \frac{(S_b - S_a)}{t * \rho} \text{ in mm}^3\text{/min;} \quad (1)$$

$$TWR = \frac{(T_b - T_a)}{t * \rho} \text{ in mm}^3\text{/min,} \quad (2)$$

where S_b, S_a are the weight of the specimen before and after machining; T_b, T_a are the weight of the tool before and after machining.

Table 1. Process parameters and their levels

S.No	Process parameters	Levels	Unit
1	Dielectric fluid	NDEDM, HCO	–
2	Tool materials	A, C, AC, CC	–
3	Al_2O_3 powder concentration	0, 1, 2, 3	g/l
4	Current	8, 16, 24, 32	A
5	Pulse on time (Ton)	10, 20, 30, 40	µs
6	Gap distance	1, 2, 3, 4	Mm

Table 2. SC and FSP process parameters

S.No	Stir casting		Friction stir processing	
1	Melting temperature	850 °C	Feed	16 mm/min
2	Stirrer type	3 arm mechanical stirrer	Tool shape	Cylindrical
3	Stirring speed	1000 rpm	Stirring speed	2000 rpm
4	Stirring time	600 s	Tilt angle	2°
5	Flux	K_2TiF_6	Shoulder and pin diameter	25 mm and 10 mm
6	Crucible	Graphite	Back plate	Mild steel
7	Reinforcement	Tungsten carbide	Reinforcement	Tungsten carbide
8	Reinforcing percentage	5 %	Reinforcing percentage	5 %

3. RESULTS AND DISCUSSION

3.1. Microstructure of the composites

The efficacy of the machining is heavily impacted by the dispersion of reinforced particles over the matrix material; thus, it is very important to check the uniform distribution of composites. For both the SC and FSP composites, as shown in Fig. 4, the SEM micrograph demonstrated the homogenous distribution of reinforcing particles. It was observed that the volume of WC particles present in the FSP was higher than the SC composites. The density of the FSP composites increases with the addition of WC particles attributed to the following facts: 1) higher density of reinforcing particles, 2) as observed in the micrograph more volume of WC particles were added to the composites which contributes to the overall increase in density.

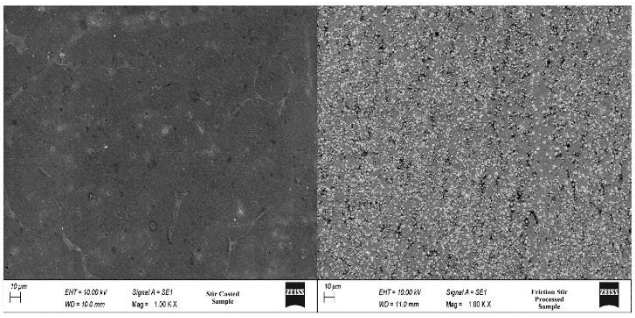

a b

Fig. 4. SEM image showing uniform distribution of composites a – SC sample; b – FSP sample

3.2. Impact of distinct process parameters on MRR

From Fig. 5, MRR values indicated that the NDEDM process resulted in a higher MRR (0.238 mm^3/min) compared to the hydrocarbon oil EDM process (0.182 mm^3/min). HCO has higher thermal conductivity (125 W/m-K) compared to NDEDM which prevent excessive heat generation results in the lower MRR. In NDEDM enhancement in MRR was accredited to the ensuing verities, 1) the lower thermal conductivity leads to localized heating, grades in higher MRR which occurred due to the high-intensity electrical discharges that generate intense heat at the interaction zone between the electrode

and the workpiece [33]; 2) the lower dielectric constant of air facilitates the localized discharges, leads to higher energy concentration [34] resulting in a higher MRR. From the results it was confirmed that dielectric fluid has a significant impact on the MRR for different tool materials. NDEDM possess low viscosity which facilitate rapid removal of debris from the spark gap. In the case of the aluminium composites tool, the near dry EDM with NDEDM dielectric fluid results in the highest MRR. When copper or copper composites were used as the electrode, owing to their high thermal conductivity, a major percentage of engendered heat was observed by the tool materials, resulting in a lower MRR. The bonding strength between the matrix and reinforcement in composite tools affects the MRR in EDM [35]. The aluminium composite tool developed through stir casting tends to exhibit a stronger bonding interface due to the molten aluminium matrix infiltrating and surrounding the reinforcement particles. This strong bonding facilitates efficient energy transfer and material removal during EDM, leading to a higher MRR. On the other hand, the bonding strength in the copper composite tool produced via friction stir processing was comparatively weaker, potentially reducing the efficiency of energy transfer and resulting in a lower MRR [36].

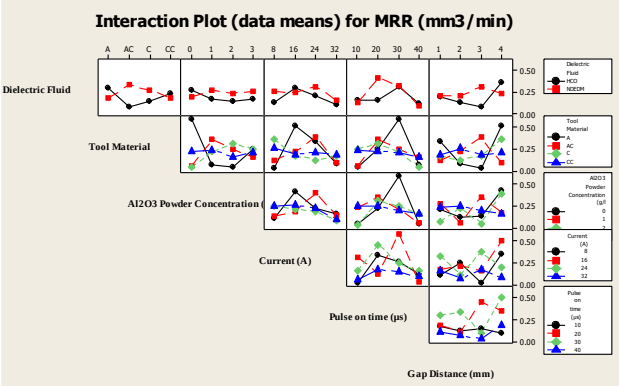

Fig. 5. Impact of process parameter on MRR of composites

When Al_2O_3 was added to the NDEDM, it increased the electrical conductivity of the medium which facilitated the formation of more stable and intense electrical discharges amid the tool and sample. The increased discharge intensity leads to higher energy transfer, resulting in an increased MRR. When the concentration level exceeds 1 g/l, owing to its insulating nature, it acts as a physical barrier between the electrode and workpiece which hinders the formation of efficient plasma channels and reduces the concentration of discharge energy at the machining zone [37]. The insulating effect can lead to slower material removal and a lower MRR. In the case of HCO, the addition of Al_2O_3 reduces MRR, contradictory to the findings of other researchers [38 – 40]. Its addition increases the viscosity of the fluid, as a result, effective removal of debris and eroded material from the machining zone becomes less efficient and reduces MRR. The optimal MRR of 0.269 mm^3/min was observed for the 20 A current, beyond which it decreases due to unstable electrical discharges. A similar trend was followed for Ton, as MRR increases until 30 µs, further increment hinders MRR attributed to the densification of the plasma channel. A wider gap distance facilitates more effective cooling and flushing of the machining debris. The wider gap allows dielectric fluid to flow and ferry away eroded particles and detritus [41]. This prevents redeposition of debris and provides better flushing conditions, which results in higher MRR.

3.3. Impact of distinct process parameters on TWR

From Fig. 6, it was inferred that the electrode possesses lower TWR when machined under HCO in comparison with NDEDM. It was attributed to the following factors: 1) HCO produces effective lubrication and acts as a coolant which reduces localized heating at the tool – material interface [42]; 2) HCO with high dielectric strength demands higher electrical voltages for breaking down, which reduces sparking frequency and hence requires more time to complete one cycle [43], resulting in reduced TWR. The observed discrepancies in TWR for different tool materials in hydrocarbon and near dry dielectric mediums can be attributed to the combined effects of dielectric fluid characteristics and tool material qualities. The usage of composites, whether in aluminium or copper, often enhances wear resistance compared to their pure counterparts, resulting in lower TWR values. Furthermore, the inclusion of a traditional dielectric fluid, such as hydrocarbon oil, helps to lower TWR values due to its cooling and lubricating qualities [44]. Due to the lack of lubricating effects, near dry EDM has slightly higher TWR values. The TWR values for hydrocarbon dielectric fluid indicate that it tends to provide lower TWR compared to near dry EDM. Hydrocarbon fluids typically possess good lubricating and cooling properties, which can reduce friction and dissipate heat during the EDM process. This lubrication and cooling effect can contribute to lower tool wear rates [45].

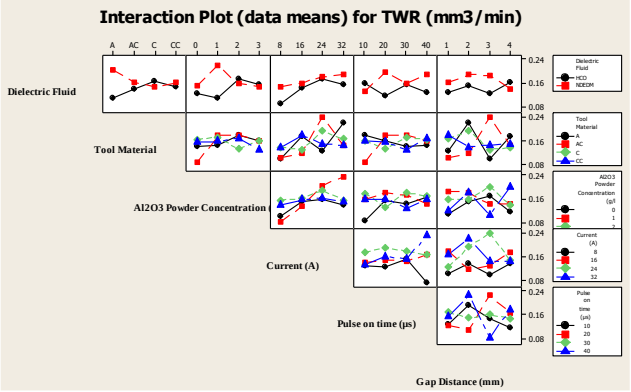

Fig. 6. Impact of process parameter on TWR of composites

In EDM, the electrical discharge generates intense heat that melts and vaporizes the workpiece material. As the current increases, the energy input also increases, leading to higher temperatures at the tool-workpiece interface. Initially, the increased energy input can result in more efficient material removal, leading to an increase in TWR. However, at higher current levels, excessive thermal effects can cause thermal damage to the tool, leading to a decline in TWR. Considering the Ton, TWR drastically increases from 0.145 mm^3/min to 0.156 mm^3/min when there is a change in Ton from 10 µs to 20 µs, beyond that no significant changes in TWR were observed. At lower Ton, the generated heat

was held inside the spark gap for a smaller period resulting in lower TWR which indicates that the energy input and material removal efficiency are relatively stable within this range [46]. From the graph, it was inferred that the TWR reaches its peak at a gap distance of 2 mm and then declines. As the gap distance increases beyond 2 mm, the heat dissipation improves, leading to lower temperatures and reduced tool wear, resulting in a decline in TWR. At a lower gap distance owing to the improver flushing and poor heat dissipation, a high TWR was recorded.

3.4. Impact of distinct process parameters on R_a

Dielectric fluids with higher dielectric strength can provide better electrical insulation and stability during EDM. This can result in more controlled and stable discharges, reducing the electrical arcing and leading to the elimination of surface irregularities [47]. Hence, specimens machined with HCO result in lower surface roughness compared to near dry EDM as shown in Fig. 7. In EDM, hydrocarbon dielectric fluid serves as a coolant, absorbing heat created during the machining process. The cooling effect aids the maintenance of steady machining conditions and reduces thermal damage [48]. The absence of a cooling medium in near dry EDM leads to insufficient heat dissipation, resulting in higher temperatures at the tool-workpiece interface. High temperatures can have a negative impact on surface quality, resulting in increased surface roughness. The specimen machined with HCO dielectric medium proffers lower surface roughness values for all tool materials compared to the NDEDM. This can be attributed to the lubricating and cooling properties of the hydrocarbon oil, which maintains uniform heat dissipation during the machining process. The better lubrication and cooling contribute to smoother surface finishes and lower surface roughness. The absence of a liquid dielectric can result in less effective lubrication and cooling, leading to heat accumulation, and potential surface irregularities [49].

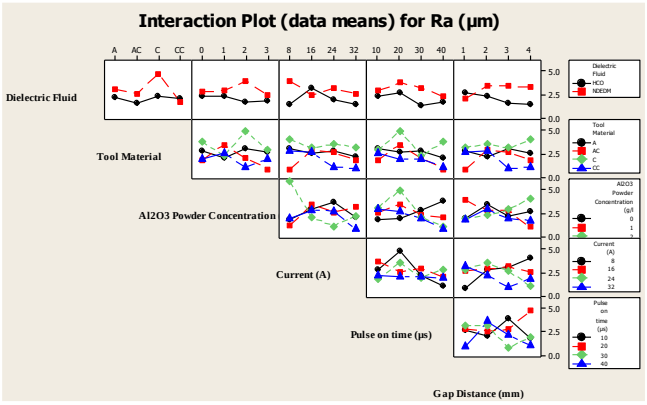

Fig. 7. Impact of process parameter on TWR of composites

The contrasting results between the two dielectric fluids can be attributed to the distinct properties of the dielectric fluid. For the NDEDM, owing to the localized heating and lower dielectric constant, a spark of high intensity struck the surface resulting in the surface of higher R_a. In the case of HCDM, as discussed in the MRR section, owing to its high thermal conductivity and density more heat was removed from the surface resulting in a smoother surface [50]. The trend showed that R_a reduces with raise in current, at higher levels it generates heat of very high intensity which produces finer debris (further investigation required) and eliminates the re-casted layer resulting in a lower R_a value. At Ton of 10 µs, heat of lower intensity was generated, hence lower MRR, and the removed debris was completely flushed away resulting in a lower R_a. For the 20 µs Ton, the machined debris was not completely flushed leading to poor surface quality. At the higher levels of Ton, generated heat was held inside the spark gap for an extended period, resulting in extreme vaporization and formation of finer debris, hence smoother surface was produced. Increasing the gap distance facilitates more space for effective flushing of removed debris from the machining gap, hence preventing re-deposition on the workpiece surface, contributing to an improved surface finish.

3.5. Surface topography

The surface topography of AA7050 composites machined in A tool under NDEDM resembled a cluster of islands separated by the lower valleys as depicted in Fig. 8 a which confirmed the localized melting. The texture also showed large numbers of globules ranging from 25 – 30 µm, revealing that the machined debris was not completely flushed away from the surface. A unique Psoriasis-like surface was observed which confirmed the occurrence of localized overheating. The texture didn't show any black blotches that had formed from the carbon content's deposition. At a higher magnification of 1000^X, the texture showed globules, cracks, craters, and irregular surface owing to poor heat dissipation as depicted in Fig. 8 b.

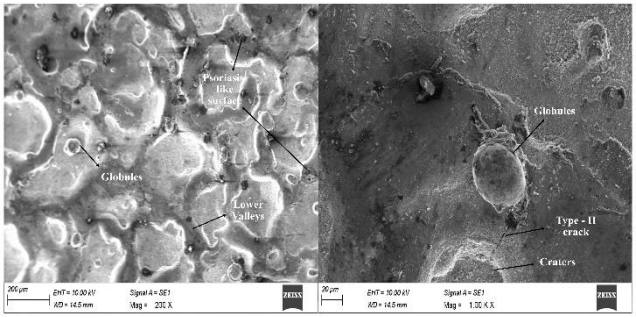

Fig. 8. Surface topography of AA7050 hybrid composites machined at NDEDM using A tool: a – at 200^X; b – at 1000^X

A micro crack of length 30 µm was observed which originated from the surface ends in a crater typically characterized as a type II crack [51]. When machined with AC, the surface texture mimics the surface of the sea with powders speared over it as shown in Fig. 9 a. The improvement in surface quality was attributed to the thermal conductivity of the AC tools which facilitates the uniform heat distribution. The globules of size less than 20 µm were observed on the surface which confirmed consistent spark distribution. Type I crack was observed which started from a common point and penetrated through the surface. At higher magnification, globules and craters were observed as depicted in Fig. 9 b.

The surface texture was smoother in comparison with the AA7050 surface machined with A. The machined debris was speared over the surface which ratifies the insufficient flushing of machined particles.

When machined with C tool under conventional EDM dielectric medium, the surface resembles the telescopic image of moon as portrayed in Fig. 10 a. The surface texture showed globules, craters, pock marks and micro cracks.

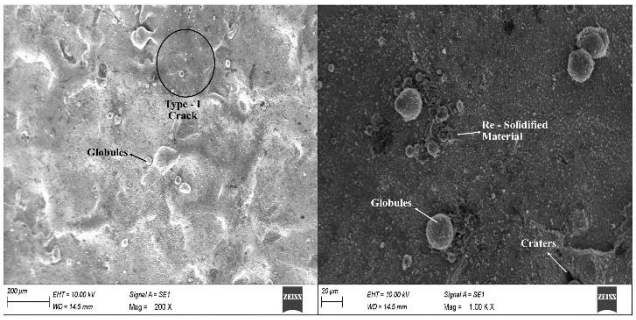

Fig. 9. Surface topography of AA7050 hybrid composites machined at NDEDM using AC tool: a – at 200^X; b – at 1000^X

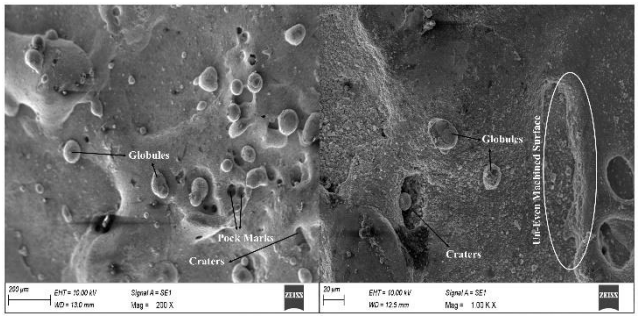

Fig. 10. Surface topography of AA7050 hybrid composites machined at EDM using C tool: a – at 200^X; b – at 1000^X

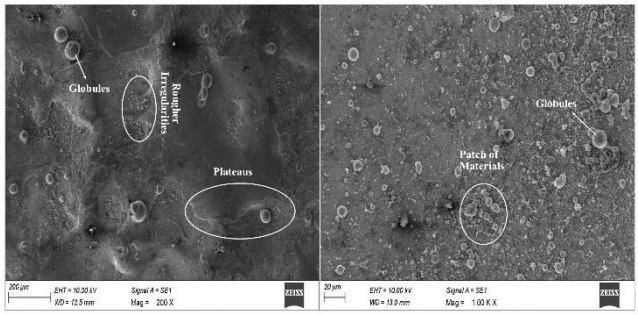

Fig. 11. Surface topography of AA7050 hybrid composites machined at EDM using CC tool: a – at 200^X; b – at 1000^X

The formation of pock marks affirmed that the vaporization occurred, as it is formed owing to releasing of entrapped gasses. The craters were formed owing to the bombardment and globus avowed that machined debris was not completely flushed away. At higher magnification, the topography showed deeper craters and uneven machined surfaces owing to the uncontrolled discharge sparks as shown in Fig. 10 b. The surface topography of specimens machined with CC resembles the plateau like features as depicted in Fig. 11 a. The surface was flat and interspersed with depression which was characterized as a relatively smoother area separated by rougher irregularities. A surface with micro pits and globules were clearly visible over the surface. The irregular area was further magnified to study the characterization of the surface as depicted in Fig. 11 b. It showed remelted particles and globules of distinct size, the patch of material sticking over the surface, removal of it leads to craters, characterized as intense sparking.

3.6. Technique for order preference by similarity to ideal solution (TOPSIS)

The TOPSIS optimisation method was used to choose the optimal rum. The initial stage is to develop a decision matrix in the optimisation approach [52]. For the present investigation, a decision matrix of 32 by 3 was formed. Eq. 3 was used to determine the normalisation of the matrix, and Table 3 shows its results:

$$Aij = \frac{\text{Yij}}{\sum_{i=1}^{n}\sqrt{(Yij)^2}} \ldots \quad (3)$$

$$Wij = wj * Aij \ldots \quad (4)$$

where i characterizes the number of variables; j characterizes the quantity of response.

The following stage included creating a weighted, normalized choice matrix, as portrayed in Eq. 4, wherein the Eigen values (△+, △-) could be calculated [53]. Where the weights (wj) of the MRR, TWR, and R_a are 0.35, 0.30, and 0.35, respectively. As indicated in Eq. 5 and Eq. 6, △+ and △- represent the extreme and least values of a weighted, normalized choice matrix for legatee attributes, respectively:

for Legatees

$$\triangle^{+} = Max\,(Wij)_{i=1}^{n},\ \ \triangle^{-} = Min\,(Wij)_{i=1}^{n}; \quad (5)$$

for Non- Legatees

$$\triangle^{+} = Min\,(Wij)_{i=1}^{n},\ \ \triangle^{-} = Max\,(Wij)_{i=1}^{n}. \quad (6)$$

Eq. 7 is used to determine the ideal (B+) and non-ideal (B-) solutions. The corresponding Euclidean distances, as shown in Eq. 8 and their values shown in the table, define the variations between the ideals and the non-ideals.

$$(B^{+}, B^{-}) = \sum_{j=1}^{n}\sqrt{(Wij - \triangle^{+})^2 + (Wij - \triangle^{n})^2}\,; \quad (7)$$

$$P^{i} = \left(\frac{D^{-}}{D^{+}+D^{-}}\right). \quad (8)$$

The process parameters 32 A current, 30 µs Ton, 3 mm gap distance machined under 3 g/l Al_2O_3 incorporated hydrocarbon oil dielectric medium using copper composites tool proffers optimal machining performance.

4. CONCLUSIONS

In this research work NDEDM and EDM of AA7050 hybrid composites were conducted, the research explores the different tool materials, such as aluminum composites and copper composites, and their influence on MRR and R_a. The investigation of distinct Al_2O_3 powder concentration in the dielectric fluid has revealed its role in altering tool wear rates and surface roughness, shedding light on the potential for optimizing EDM performance through tailored powder concentrations. The study of dielectric fluid properties, including viscosity and dielectric strength, has further contributed to a deeper comprehension of their influence on process outcomes.

Table 3. Optimization of parameters using the TOPSIS technique

Normalised matrix			Weighted normalised matrix			*D+*	*D-*	Assessment value	Rank
0.00098	0.00838	0.0717	0.000322	0.00276458	0.02438	0.131685956	1.051952183	0.88874475	10
0.00637	0.04893	0.46607	0.00210126	0.01614791	0.15846	0.201482667	0.917649045	0.81996519	19
0.00742	0.03866	0.07902	0.00244734	0.01275868	0.02687	0.130595422	1.049280391	0.88931426	8
0.02308	0.01774	0.07205	0.00761793	0.00585325	0.0245	0.124610675	1.051793703	0.89407496	4
0.06938	0.03554	0.34541	0.02289506	0.01172655	0.11744	0.156759265	0.95900473	0.859505	14
0.04919	0.02806	1.04519	0.01623408	0.00926	0.35537	0.369620476	0.721086351	0.6611184	28
0.00539	0.01307	0.06608	0.00177941	0.00431394	0.02247	0.130002284	1.053828533	0.89018508	6
0.3951	0.02117	0.01157	0.13038284	0.00698463	0.00393	0.006944908	1.080199514	0.99361179	1
0.0012	0.00012	0.48692	0.00039546	3.9719E-05	0.16555	0.207405288	0.910900403	0.81453614	21
0.00269	0.0311	0.12245	0.00088916	0.01026299	0.04163	0.135256954	1.034549726	0.88437666	12
0.04472	0.01275	0.15956	0.01475896	0.00420626	0.05425	0.126166822	1.022159849	0.89012985	7
0.00055	0.02693	0.52844	0.00018025	0.0088857	0.17967	0.218893753	0.896561621	0.80376288	24
0.03099	0.02532	0.52368	0.01022525	0.00835433	0.17805	0.211716921	0.898249584	0.80925828	22
0.00789	0.02169	0.05277	0.00260274	0.00715617	0.01794	0.128742286	1.058298066	0.89154346	5
0.02152	0.05001	0.45971	0.00710307	0.01650176	0.1563	0.196684876	0.919831905	0.82384065	17
0.00209	0.01007	0.37957	0.00068862	0.00332273	0.12906	0.180240448	0.947292515	0.84014618	16
0.27597	0.07972	0.41038	0.09107039	0.02630849	0.13953	0.143601109	0.940932782	0.86759187	13
0.0969	0.02369	1.0585	0.03197691	0.00781927	0.35989	0.369390898	0.717130939	0.66002441	29
0.02522	0.01817	0.53938	0.00832107	0.00599502	0.18339	0.217115366	0.892946388	0.80441145	23
0.03935	0.0355	0.02131	0.01298649	0.01171531	0.00725	0.118021996	1.068990052	0.9005722	3
0.01064	0.01966	0.11994	0.00350997	0.00648624	0.04078	0.132272203	1.035478346	0.88672906	11
0.00058	0.03375	0.06482	0.0001925	0.01113618	0.02204	0.131910925	1.054127048	0.88878018	9
0.05816	0.02408	0.07683	0.01919165	0.00794719	0.02612	0.113659046	1.050273778	0.90234914	2
0.09795	0.02272	0.67298	0.032325	0.0074966	0.22881	0.245441371	0.848078391	0.77554921	25
0.00423	0.08284	0.47022	0.00139649	0.027337	0.15987	0.204205551	0.916169822	0.8177347	20
1.4E-06	0.03803	0.4511	4.4691E-07	0.01254826	0.15337	0.198716386	0.922787759	0.82281262	18
0.03049	0.0479	1.28547	0.01006172	0.0158066	0.43706	0.449802604	0.639167732	0.58694687	31
0.00162	0.03237	0.32635	0.00053485	0.01068051	0.11096	0.168606807	0.965226807	0.85129493	15
0.02623	0.0396	1.2719	0.00865551	0.01306687	0.43245	0.445657002	0.643812684	0.59094135	30
0.15898	0.01574	0.79534	0.05246391	0.00519478	0.27041	0.277686609	0.807638166	0.74414423	27
0.05908	0.01152	3.16483	0.01949789	0.00380263	1.07604	1.077834326	0.030561693	0.0275729	32
0.05908	0.01152	0.66744	0.01949789	0.00380263	0.22693	0.24907095	0.849663727	0.7733111	26

1. The specimens machined with NDEDM proffer high MRR and TWR compared to hydrocarbon oil. HCO demonstrated a better surface finish with lower Ra values, making it suitable for applications where smooth surfaces are a priority.
2. Samples machined with AC exhibited the highest MRR, making it an excellent choice for roughing operations. In contrast, CC tools provided superior surface finish with lower Ra values, indicating their suitability for precision finishing tasks. For roughing operation, it is recommended to machine with the combination of AC and NDEDM and for smoothing operation it was CC and EDM.
3. Al_2O_3 powder addition in the dielectric fluid enhanced MRR and improved the surface finish. Craters, globules, pock marks, psoriasis like structures, remelted layers and micro cracks are the distinct features observed on the surface topography.
4. The optimum machining performance is provided by the process settings of 32 A current, 30 µs Ton, 3 mm gap spacing, 3 g/l Al_2O_3 integrated with hydrocarbon oil dielectric medium, and copper composite tool.

REFERENCES

1. **Somu, C., Ranjith, R.** Electric Discharge Machining of Inconel 718 Under a Distinct Dielectric Medium *ECS Journal of Solid State Science and Technology* 11 (5) 2022: pp. 053010. https://doi.org/10.1149/2162-8777/ac6d77
2. **Ho, K.H., Newman, S.T.** State Of The Art Electrical Discharge Machining (EDM) *International Journal of Machine Tools and Manufacture* 43 (13) 2003: pp. 1287 – 1300. https://doi.org/10.1016/S0890-6955(03)00162-7
3. **Prakash, T., Ranjith, R., Krishna Mohan, S., Venkatesan, S.** Electric Discharge Machining of AZ91 Magnesium Hybrid Composites under Different Dielectric Mediums *Advances in Materials Science and Engineering* 2022: pp. 01 – 15. https://doi.org/10.1155/2022/3502383
4. **Bédard, F., Jahazi, M., Songmene, V.** Die-Sinking Edm of Al6061-T6: Interactions Between Process Parameters, Process Performance, And Surface Characteristics *The International Journal of Advanced Manufacturing Technology* 107 2020: pp. 333 – 342. https://doi.org/10.1007/s00170-020-05109-z
5. **Mausam, K., Sharma, K., Bharadwaj, G., Singh, R.P.** Multi-Objective Optimization Design of Die-Sinking Electric Discharge Machine (EDM) Machining Parameter for Cnt-Reinforced Carbon Fibre Nanocomposite Using Grey Relational Analysis *Journal of the Brazilian Society of Mechanical Sciences and Engineering* 41 2019: pp. 1 – 8. https://doi.org/10.1007/s40430-019-1850-4
6. **Muthuramalingam, T., Mohan, B.** A Review on Influence of Electrical Process Parameters in EDM Process *Archives of Civil and Mechanical Engineering* 15 (1) 2015: pp. 87 – 94.

https://doi.org/10.1016/j.acme.2014.02.009

7. **Dikshit, M.K., Anand, J., Narayan, D. Jindal, S.** Machining Characteristics and Optimization of Process Parameters in Die-Sinking EDM Of Inconel 625 *Journal of the Brazilian Society of Mechanical Sciences and Engineering* 41 2019: pp. 1 – 14. https://doi.org/10.1007/s40430-019-1809-5
8. **Bhattacharya, A., Batish, A., Singh, G., Singla, V.K.** Optimal Parameter Settings for Rough and Finish Machining of Die Steels in Powder-Mixed EDM *The International Journal of Advanced Manufacturing Technology* 61 2012: pp. 537 – 548. https://doi.org/10.1007/s00170-011-3716-5
9. **Kansal, H.K., Singh, S., Kumar, P.** Effect of Silicon Powder Mixed EDM on Machining Rate of AISI D2 Die Steel *Journal of Manufacturing Processes* 9 (1) 2007: pp. 913 – 922. https://doi.org/10.1016/S1526-6125(07)70104-4
10. **Singh, B., Kumar, J., Kumar, S.** Investigation of the Tool Wear Rate in Tungsten Powder-Mixed Electric Discharge Machining of AA6061/10% SiCp Composite *Materials and Manufacturing Processes* 31 (4) 2016: pp. 456 – 466.
11. **Singh, B., Kumar, J., Kumar, S.** Influences of Process Parameters on MRR Improvement in Simple and Powder-Mixed EDM of AA6061/10% SiC Composite *Materials and Manufacturing Processes* 30 (3) 2015: pp. 303 – 312. https://doi.org/10.1080/10426914.2014.930888
12. **Ramesh, S., Jenarthanan, M.P.** Optimizing the Powder Mixed EDM Process of Nickel Based Super Alloy *Proceedings of the Institution of Mechanical Engineers, Part E: Journal of Process Mechanical Engineering* 235 (4) 2021: pp. 1092 – 1103. https://doi.org/10.1177/09544089211002782
13. **Singaravel, B., Shekar, K.C., Reddy, G.G., Prasad, S.D.** Experimental Investigation of Vegetable Oil as Dielectric Fluid in Electric Discharge Machining of Ti-6Al-4V *Ain Shams Engineering Journal* 11 (1) 2020: pp. 143 – 147. https://doi.org/10.1016/j.asej.2019.07.010
14. **Sadagopan, P., Mouliprasanth, B.** Investigation on the Influence of Different Types of Dielectrics in Electrical Discharge Machining *The International Journal of Advanced Manufacturing Technology* 92 (1 – 4) 2017: pp. 277 – 291. https://doi.org/10.1007/s00170-017-0039-1
15. **Chen, S.L., Yan, B.H., Huang, F.Y.** Influence of Kerosene and Distilled Water as Dielectrics on the Electric Discharge Machining Characteristics of Ti–6A1–4V *Journal of Materials Processing Technology* 87 (1 – 3) 1999: pp. 107 – 111. https://doi.org/10.1016/S0924-0136(98)00340-9
16. **Dhakar, K., Dvivedi, A., Dhiman, A.** Experimental Investigation on Effects of Dielectric Mediums in Near-Dry Electric Discharge Machining *Journal of Mechanical Science and Technology* 30 2016: pp. 2179 – 2185. https://doi.org/10.1007/s12206-016-0425-x
17. **Ng, P.S., Kong, S.A., Yeo, S.H.** Investigation of Biodiesel Dielectric in Sustainable Electrical Discharge Machining *The International Journal of Advanced Manufacturing Technology* 90 2017: pp. 2549 – 2556. https://doi.org/10.1007/s00170-016-9572-6
18. **Sundriyal, S., Vipin Walia, R.S.** Experimental Investigation and Performance Enhancements Characteristics of Gaseous Assisted Powder Mixed Near Dry Electric Discharge Machining *Proceedings of the Institution of Mechanical Engineers, Part E: Journal of Process Mechanical Engineering* 235 (4) 2021: pp. 1048 – 1058. https://doi.org/10.1177/0954408920988424
19. **Bai, X., Zhang, Q.H., Yang, T.Y., Zhang, J.H.** Research on Material Removal Rate of Powder Mixed Near Dry Electrical Discharge Machining *The International Journal of Advanced Manufacturing Technology* 69 2013: pp. 1757 – 1766. https://doi.org/10.1007/s00170-013-4973-2
20. **Sundriyal, S., Walia, R.S., Tyagi, M.** Investigation on Surface Finish in Powder Mixed Near Dry Electric Discharge Machining Method *Materials Today: Proceedings* 25 2020: pp. 804 – 809. https://doi.org/10.1016/j.matpr.2019.09.031
21. **Bai, X., Zhang, Q., Zhang, J., Kong, D., Yang, T.** Machining Efficiency of Powder Mixed Near Dry Electrical Discharge Machining Based on Different Material Combinations of Tool Electrode and Workpiece Electrode *Journal of Manufacturing Processes* 15 (4) 2013: pp. 474 – 482. https://doi.org/10.1016/j.jmapro.2013.09.005
22. **Khanra, A.K., Sarkar, B.R., Bhattacharya, B., Pathak, L.C., Godkhindi, M.M.** Performance of Zrb2–Cu Composite as an EDM Electrode *Journal of Materials Processing Technology* 183 (1) 2007: pp. 122 – 126. https://doi.org/10.1016/j.jmatprotec.2006.09.034
23. **Bhaumik, M., Maity, K.** Effect of Different Tool Materials during EDM Performance of Titanium Grade 6 Alloy *Engineering Science and Technology, an International Journal* 21 (3) 2018: pp. 507 – 516. https://doi.org/10.1016/j.jestch.2018.04.018
24. **Khanra, A.K., Pathak, L.C., Godkhindi, M.M.** Application of New Tool Material for Electrical Discharge Machining (EDM) *Bulletin of Materials Science* 32 2009: pp. 401 – 405. https://doi.org/10.1007/s12034-009-0058-
25. **Sharma, D., Hiremath, S.S.** Review on Tools and Tool Wear in EDM *Machining Science and Technology* 25 (5) 2021: pp. 802 – 873. https://doi.org/10.1080/10910344.2021.1971711
26. **Bhaumik, M., Maity, K.** Effect if Different Tool Materials During EDM Performance of Titanium Grade 6 Alloy *Engineering Science and Technology, an International Journal* 21 (3) 2018: pp. 507 – 516. https://doi.org/10.1016/j.jestch.2018.04.018
27. **El-Taweel, T.A.** Multi-Response Optimization of EDM With Al–Cu–Si–TiC P/M Composite Electrode *The International Journal of Advanced Manufacturing Technology* 44 2009: pp. 100 – 113. https://doi.org/10.1007/s00170-008-1825-6
28. **Tsai, H.C., Yan, B.H., Huang, F.Y.** EDM Performance of Cr/Cu-Based Composite Electrodes *International Journal of Machine Tools and Manufacture* 43 (3) 2003: pp. 245 – 252. https://doi.org/10.1016/S0890-6955(02)00238-9
29. **Singh, S., Maheshwari, S., Pandey, P.C.** Some Investigations into the Electric Discharge Machining of Hardened Tool Steel Using Different Electrode Materials *Journal of Materials Processing Technology* 149 (1 – 3) 2004: pp. 272 – 277. https://doi.org/10.1016/j.jmatprotec.2003.11.046
30. **Manivannan, R., Kumar, M.P.** Multi-Response Optimization of Micro-EDM Process Parameters on AISI304 Steel Using TOPSIS *Journal of Mechanical Science and Technology* 30 2016: pp. 137 – 144. https://doi.org/10.1007/s12206-015-1217-4
31. **Wang, Q., Liu, F., Wang, X.** Multi-Objective Optimization of Machining Parameters Considering Energy Consumption

The International Journal of Advanced Manufacturing Technology 71 2014: pp. 1133 – 1142. https://doi.org/10.1007/s00170-013-5547-z

32. **Ramesh, S., Viswanathan, R., Ambika, S.** Measurement and Optimization of Surface Roughness and Tool Wear Via Grey Relational Analysis, TOPSIS And RSA Techniques *Measurement* 2016 78: pp. 63 – 72. https://doi.org/10.1016/j.measurement.2015.09.036
33. **Baroi, B.K., Jagadish Patowari, P.K.** A Review on Sustainability, Health, And Safety Issues of Electrical Discharge Machining *Journal of the Brazilian Society of Mechanical Sciences and Engineering* 44 (2) 2022: pp. 59. https://doi.org/10.1007/s40430-021-03351-4
34. **Boopathi, S.** Performance Improvement of Eco-Friendly Near-Dry Wire-Cut Electrical Discharge Machining Process Using Coconut Oil-Mist Dielectric Fluid *Journal of Advanced Manufacturing Systems* 22 (02) 2023: pp. 339 – 358. https://doi.org/10.1142/S0219686723500178
35. **Ranjith, R., Tamilselvam, P., Prakash, T., Chinnasamy, C.** Examinations Concerning the Electric Discharge Machining of AZ91/5B (4) C (P) Composites Utilizing Distinctive Electrode Materials *Materials and Manufacturing Processes* 34 (10) 2019: pp. 1120 – 1128.
36. **Asif, N., Saleem, M.Q., Farooq, M.U.** Performance Evaluation of Surfactant Mixed Dielectric and Process Optimization for Electrical Discharge Machining of Titanium Alloy Ti6Al4V *CIRP Journal of Manufacturing Science and Technology* 43 2023: pp. 42 – 56. https://doi.org/10.1016/j.cirpj.2023.02.007
37. **Dhakar, K., Kumar, R., Katheria, A., Nagdeve, L., Kumar, H.** Effect of Various Dielectric Fluids on Electric Discharge Machining (EDM): A Review *Journal of the Brazilian Society of Mechanical Sciences and Engineering* 44 (10) 2022: pp. 487. https://doi.org/10.1016/j.cirpj.2023.02.007
38. **Ranjith, R., Prabhakar, M., Giridharan, P.K., Ramu, M.** Influence of Al_20_3 Particle Mixed Dielectric Fluid on Machining Performance of Ti6Al4V *Surface Topography: Metrology and Properties* 9 (4) 2021: p. 045052. https://doi.org/10.1088/2051-672X/ac456a
39. **Mustu, M., Demir, B., Aydin, F., Gürün, H.** An Investigation of the PMEDM Processing and Surface Characterizations of AZ61 Matrix Composites Via Experimental and Optimization Methods *Materials Chemistry and Physics* 300 2023: pp. 127526. https://doi.org/10.1016/j.matchemphys.2023.127526
40. **Shiek, J., Sairam, J., Mouda, P.A.** Parameter Optimization in the Enhancement of MRR of Titanium Alloy Using Newer Mixing Method in PMEDM Process *Journal of Engineering and Applied Science* 70 (1) 2023: pp. 1 – 16. https://doi.org/10.1016/j.matchemphys.2023.127526
41. **Rathod, R., Kamble, D., Ambhore, N.** Performance Evaluation of Electric Discharge Machining of Titanium Alloy – A Review *Journal of Engineering and Applied Science* 69 (1) 2022: pp. 1 – 19. https://doi.org/10.1186/s44147-022-00118
42. **Gattu, S.D., Yan, J.** Micro Electrical Discharge Machining of Ultrafine Particle Type Tungsten Carbide Using Dielectrics Mixed with Various Powders *Micromachines* 13 (7) 2022: pp. 998. https://doi.org/10.3390/mi13070998
43. **Arif, U., Ali Khan, I., Hasan, F.** Green and Sustainable Electric Discharge Machining: A Review *Advances in Materials and Processing Technologies* 2022: pp. 1 – 75. https://doi.org/10.1080/2374068X.2022.2108599
44. **Yadav, V.K., Singh, R., Kumar, P., Dvivedi, A.** Investigating the Performance of the Rotary Tool Near-Dry Electrical Discharge Machining Process Through Debris Analysis *Journal of Materials Engineering and Performance* 31 (10) 2022: pp. 8405 – 8417. https://doi.org/10.1007/s11665-022-06811-7
45. **Singh, M., Jain, V.K., Ramkumar, J.** 3-D Fabrication Using Electrical Discharge-Milling: An Overview *Materials and Manufacturing Processes* 37 (11) 2022: pp. 1215 – 1245. https://doi.org/10.1080/10426914.2022.2072888
46. **Zulkeflee, M.F., Dzulkifli, N.F., Mamat, A.** Water-in-Sunflower Seed Oil Emulsion as a Dielectric Fluid For Micro Electrical Discharge Machining (μEDM) *Matéria (Rio de Janeiro)* 27 (4) 2022: pp. 01 – 16. https://doi.org/10.1590/1517-7076-RMAT-2022-0208
47. **Jain, N., Jain, J.K., Harane, P.P., Unune, D.R.** Application of a Novel Non-Edible Oil-Based Water-in-oil Nano-Emulsion as a Dielectric for the Amelioration of Electrical Discharge Machining Performance *Journal of the Brazilian Society of Mechanical Sciences and Engineering* 45 (7) 2023: pp. 379. https://doi.org/10.1007/s40430-023-04302-x
48. **Rafaqat, M., Mufti, N.A., Ahmed, N., Rehman, A.U., AlFaify, A.Y., Farooq, M.U., Saleh, M.** Hole-Making in D2-Grade Steel Tool by Electric-Discharge Machining through Non-Conventional Electrodes *Processes* 10 (8) 2022: pp. 1553. https://doi.org/10.3390/pr10081553
49. **Sethy, S., Behera, R.K., Muduli, K., Kandasamy, J., Davim, J.P., Rana, J.** Bio-Dielectrics to Improve the Performance of Electro Discharge Machining – An Investigation for Cleaner Production Opportunities *Advances in Materials and Processing Technologies* 2023: pp. 1 – 20. https://doi.org/10.1080/2374068X.2023.2215607
50. **Shastri, R.K., Mohanty, C.P., Dash, S., Gopal, K.M.P., Annamalai, A.R., Jen, C.P.** Reviewing Performance Measures of the Die-Sinking Electrical Discharge Machining Process: Challenges and Future Scopes *Nanomaterials* 12 (3) 2022: pp. 384. https://doi.org/10.3390/nano12030384
51. **Jayachitra, R., Ranjith, R., Ramesh, B., Lawanya, R.** Surface Modification of Hastelloy Processed by the Cu Mixed Electric Discharge Alloying Technique *Surface Engineering* 38 (5) 2022: pp. 482 – 498. https://doi.org/10.1080/02670844.2022.2106312
52. **Corrente, S., Tasiou, M.** A Robust TOPSIS Method For Decision Making Problems with Hierarchical and Non-Monotonic Criteria *Expert Systems with Applications* 214 2023: pp. 119045. https://doi.org/10.1016/j.eswa.2022.119045
53. **Ranjith, R., Vimalkumar, S.N.** Integrated MOORA-ELECTRE Approach for Solving Multi-Criteria Decision Problem *World Journal of Engineering* 19 (4) 2022: pp. 510 – 521. https://doi.org/10.1108/WJE-12-2020-0656